CHAPTER 6

Upconverting Fluorescent Nanoparticles for Biological Applications

I. Amalraj Appavoo[1] and Y. Zhang[1,2]

[1]*Nanoscience and Nanotechnology Initiative, National University of Singapore, Singapore*

[2]*Division of Bioengineering, Faculty of Engineering, National University of Singapore, Singapore*

CONTENTS

ABSTRACT

Fluorescent labelling is widely used as an indispensable tool in biology for the study of complex molecular interactions. Conventional downconversion fluorescence labels with ultraviolet (UV) or short wavelength excitation suffer from the presence of autofluorescence, low signal-to-noise ratio and incident photodamage to living organisms. This chapter focuses on upconverting fluorescent nanoparticles with excitation in near-infrared region. This has several advantages including very low autofluorescence, absence of photodamage to living organisms, high detection sensitivity and high light penetration depth.

Emerging Nanotechnologies for Manufacturing

6.1 INTRODUCTION

Most biomolecules lack sensitive detectable fluorescent signal; hence there is a need for fluorescent labels to study their molecular interactions. Fluorescent probes emit fluorescence at certain wavelengths which can be detected using fluorescence microscope under in vitro and in vivo conditions. Exogenous labels for biological analysis were first introduced by American scientists Yalow and Berson in the form of radioimmunoassay (RIA). Apart from its high sensitivity (10^{-9}–10^{-12}) and wide application, it suffers from radioactivity and inherently short half-life. This has led to the introduction of various non-radioactive labelling techniques based on enzyme-catalysed reactions, bio/chemiluminescence and fluorescence. Of the three, fluorescent labelling is widely used in biology and medicine. Fluorescence is the luminescence phenomenon that occurs in fluorophores. It is a process by which a fluorophore absorbs particular wavelength of light and excites to higher energy state with emission of light. This emission energy corresponds to the energy difference between excited state and ground state. The optical properties of fluorophores such as fluorescence intensity, excitation spectrum, emission spectrum and fluorescence lifetime help to encode the happenings around the molecule that is monitored. For example, labels which are environmentally sensitive can be used as molecular reporters. Information on what is happening in their molecular environment can thus be derived from their fluorescence signals, and their exact locations can be monitored using fluorescence microscopy. Most of the conventional fluorescent labels follow the principle of Stokes law. They are excited under UV or short wavelength excitation. The main problems in using them are: autofluorescence (noise) from the analytes under UV and short wavelength excitation which decreases the signal-to-noise ratio, low light penetration depth and severe damage to living organisms[1–3]. Some conventional fluorescent labels used are organic dyes, fluorescent proteins, lanthanide chelates, semiconductor quantum dots (QDs), lanthanide doped inorganic nanoparticles and fluorophoretagged latex/silica nanobeads. However, the most commonly used are organic dyes and QDs.

Organic dyes, though popular owing to their low cost, availability and easy usage, also pose some challenges such as short Stokes shift, poor photo-chemical stability, susceptibility to photobleaching and decomposition under repeated excitation. However, recent research has overcome some of these problems. Some commonly used organic dyes are fluorescein, rhodamine, cyanine and Alexa dyes. QDs are semiconductor nanoparticles composed of atoms from groups II–VI or III–V of the periodic table. They are generally defined as particles having physical dimensions smaller than the exciton Bohr radius, typically 1–5 nm. This small size leads to a quantum

confinement effect, which endows nanoparticles with unique optical and electronic properties. Advantages of using QDs over other fluorescent labels include great assay sensitivity and stability and better emission selectivity. QDs with different sizes and compositions can be excited simultaneously with a single wavelength of light to produce emissions at different wavelengths useful in multiplex detection studies. Again QDs are not foolproof. Major problems involve presence of autofluorescence and toxicity. These obstacles in the application of conventional labels have paved the way to develop a new class of labelling materials.

Upconverting nanoparticles (UCN) with near-infrared (NIR) excitation are the best choice. The process in which the emission energies are found to exceed excitation energies by 10–100 times *KT* violating Stokes law in its basic statement is called upconversion (UC). Coupled lanthanide and uranide f ions and transition metal d ions, when embedded in solids, produce UC fluorescence under moderate to strong excitation density. UCN convert low energy exciting photons to visible emissions. They have various advantages such as absence of autofluorescence and of photodamage to living organisms as exciting NIR light does not excite the biological samples; deep tissue penetration as NIR light shows low scattering effect; high emission signals as the UC process occurring inside the host materials is not affected by external environment such as pH, temperature, etc.; multiplex imaging as under same excitation, the emission wavelengths of UCN can be varied by changing their doping ions[4, 5]. This chapter gives an overview of UCN and their bioapplications.

6.2 THE MECHANISM OF FLUORESCENT UC

A wide variety of mechanisms have been proposed for the occurrence of UC either alone or in combinations of absorption and non-radiative energy transfer steps. Absorption is in two basic forms, that is, the ground state absorption (GSA) – promotion of ions from its ground state to an excited state – and the excited state absorption (ESA) – promotion of ions from its excited state to a higher excited state – as shown in Figure 6.1a. Non-radiative energy transfer may take place between either like energy levels or unlike energy levels. Energy transfer among like levels of like ions is the common phenomenon of energy migration.

A similar process between unlike ions may lead to energy trapping or sensitization effect. Energy transfer between unlike levels may result in energy transfer upconversion (ETU) and cross relaxation (CR). ETU is a process in which a low lying neighbour donates its excitation energy to a neighbouring excited ion which is then promoted to a higher excited state. Figure 6.1b

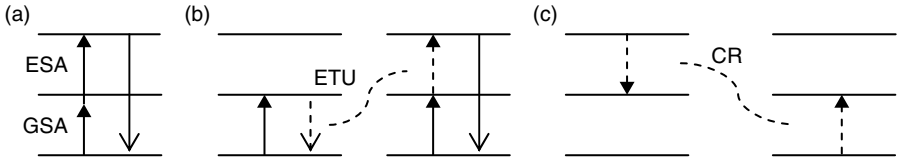

FIGURE 6.1 *Upconversion mechanism: (a) ground state absorption followed by excited state absorption (GSA/ESA); (b) ground state absorption followed by energy transfer upconversion (GSA/ETU); (c) Cross relaxation (CR).*

shows the mechanism of GSA followed by ETU. ETU is inherently a pairwise or multicentre effect which strongly depends upon concentration of ions. CR is the reverse of ETU. In CR, an ion (at higher excited levels) is partially deactivated through energy transfer to a ground state neighbour, with both ions at lower excited levels, as shown in Figure 6.1c.

6.3 UPCONVERTING NANOPARTICLES

UC occurs in various ion-doped solids such as crystals[6, 7] and glasses[8–11]. Usually lanthanide (4f), actinide (5f) and transition metal (3d, 4d, 5d) ions can produce UC fluorescent emission when embedded in solids or organic ligand. Of these, trivalent lanthanides based UC are predominantly used. This is because lanthanides have more than one metastable state (except Yb^{3+}) which makes them best suited for UC. This is due to the fact that the spectroscopically active 4f electrons are well shielded from their chemical environment by the outer-lying 5s and 5p electrons, resulting in particularly small electron–phonon coupling strength for various excited f–f states. As a consequence, luminescence processes are much more competitive with multiphonon relaxation in lanthanides compared to other ions, and their excited lifetime is typically in the range of 10^{-6}–10^{-2} s. Also, in lanthanide centred f–f transitions, there is only a small displacement between the ground state and the excited state. Lanthanide ions, Pr^{3+}, Nd^{3+}, Dy^{3+}, Ho^{3+}, Er^{3+}, Yb^{3+}, Sm^{3+} and Tm^{3+}, have been used widely for synthesis of UC fluorescent materials[12–14]. Transition metal based UC is considerably less explored due to the much stronger electron–phonon coupling of d-electrons, which leads to dominant non-radiative relaxation based on multiphonon processes for most of the excited d–d states. Some examples are Ti^{2+}, Ni^{2+}, Mo^{3+}, Re^{4+} and Os^{4+} doped halides[15–20].

The principal strategies for obtaining new inorganic UC nanoparticles involve changing the host lattice and doping ions. Changing the host lattice may dramatically influence the radiative and non-radiative (multiphonon

Table 6.1 List of Examples of Upconverting Inorganic Nanoparticles

Host Material	Absorber Ion	Emitter Ion	Emission(s)	Wavelength (nm)	Reference
YF_3	Yb	Er	Blue	411	[28]
GdF_3	Yb	Er	Green, red	520–550, 665	[29]
$NaYF_4$	Yb	Er, Tm	Green, red, blue	518–545, 652–655, 475	[30]
LaF_3	Yb	Er, Tm, Ho	Green, blue, red	545, 475.2, 657.8	[31]
Y_2O_2S	Yb	Er, Ho, Tm	Green, red	520–580, 650–700	[26]
			Green, red	550, 640–680	
			Blue, red	460, 640–680	
Gd_2O_2S	Yb	Er	Green, red	520–580, 650–700	[32]
Y_2O_3	Yb	Er	Red	662	[21]
$La_2(MoO_4)_3$	Yb	Er	Green, red	519–541, 653	[33]
ZnO		Er	Green	520–550	[34]
Gd_2O_3	Yb	Er	Green, red	520–580, 650–700	[32]
Y_3NbO_7	Er		Green, red	550, 665	[35]
Lu_2O_3	Yb	Ho	Green, red	548, 667	[36]
$Cs_2NaGdCl_6$	Tm	Ho	Blue, green	492, 543	[37]
			Yellow, red	588, 657	

relaxation as well as energy transfer) properties, leading to entirely different UC luminescence behaviour. For example, one can reduce the efficiency of multiphonon[21] relaxation processes by changing the lattice from high phonon energies (fluoride, oxide, etc.)[22–26] to low phonon energies (chlorides, bromides, iodides, etc.)[16, 18]. But most of these low phonon energy lattices are hygroscopic. Choosing a host with specific optical and/or magnetic properties may also influence the UC emission properties of a dopant ion through sensitization or perturbation by exchange interactions[27]. Similarly, a change in dopant ions has dramatic effect on UC emission. The most obvious effect is the change in emission wavelength. The choice of host lattice and co-dopant covers a very broad range of possibilities in the development of compounds with new and unprecedented UC properties, leaving much to the imagination and creativity of the researcher. Some upconverting nanocrystals are summarized in Table 6.1.

Usually lanthanide cations show very weak absorption that extensively decreases their emission. This drawback is overcome in coordination chemistry by the development of 'antenna effect'. This allows an increase in luminescence intensity through indirect excitation by tuning the absorption cross sections into regions unabsorbed by the nanoparticles. Some examples are: energy

transfer to lanthanide cations from anions present in bulk structure of phosphate and vanadate based nanoparticles; energy transfer from surface passivating shells in SiO_2 coated nanoparticles; capping chromogenic ligands[38–40].

6.4 CONJUGATION OF BIOMOLECULES TO UCN

For bioapplications, UCN should be hydrophilic, biocompatible and should possess functional groups to facilitate covalent bioconjugations[30]. Most of UCN are synthesized in organic solvents[5, 41, 42] or at high temperatures[30, 33]. Organic surfactants such as cetyl-trimethylammonium bromide (CTAB) or ethylenediamine tetra acetic acid (EDTA) are often used as ligands to control the particle growth and stabilization against aggregation resulting in a hydrophobic surface. Hence, surface modification is required for these UCN before employing them in biological studies[30, 43]. The surface modification is much dependent on surface chemistry of UCN; so, it is difficult to achieve all desired properties using one universal method.

The surface modification of UCN is made by coating a thin layer of either silica or polymer. Silica coating is an attractive method, as their surface chemistry is well documented[44–47]. The surface silica prevents nanoparticles from flocculation and provides room for decoration with functional groups such as thiol, amino and carboxyl groups, which allow greater control in conjugation protocols[48]. On the other hand, hydrophilic, biocompatible and bifunctional polymers are used as chelating and stabilizing agents for UCN. They render the surface of UCN hydrophilic and provide functional groups for bioconjugations. The polymers such as polyvinylpyrrolidone[49] chitosan[50–52], polyethylenimine (PEI)[49, 53], poly(acrylic acid)(sodium salt)(PAAcNa)[54] and polyethylene glycol (PEG)[55] are used for synthesis of UCN. The presence of polymer does not affect the fluorescence spectrum of polymer/UCN. Figure 6.2 shows the fluorescence spectrum of PEI/$NaYF_4$:Yb^{3+}, $Ln3^+$ (Ln: Er or Tm) nanoparticles. Also, further increase in functionality can be achieved by encapsulating polymer/UCN with a uniform layer of silica. The schematic representation of silica/PVP stabilized nanoparticles[49] is shown in Figure 6.3.

6.5 UCN FOR BIOLOGICAL APPLICATIONS

6.5.1 UCN in immunoassays

The immunoassay is used to measure the concentration of substance in biological liquid (serum or urine) using the bio-affinity between antibody and antigen. It has important applications in the diagnosis of infectious and genetic diseases. Labelling the antibody or antigen is commonly used

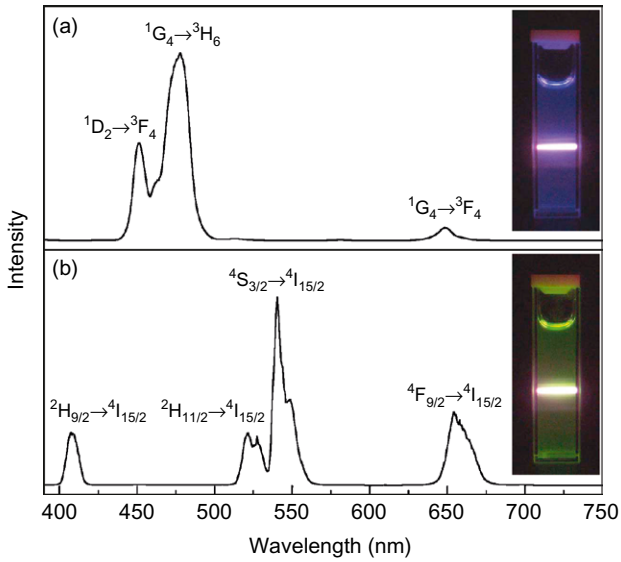

FIGURE 6.2 *NIR-to-visible UC fluorescence spectra and photographs of the (a) PEI/$NaYF_4$:Yb^{3+}, Tm^{3+} and (b) PEI/$NaYF_4$:Yb^{3+}, Er^{3+} nanoparticles in aqueous solutions (1 mg mL^{-1}) excited at 980 nm using an NIR laser.*

Source: Reproduced with permission from Ref. [53], IOP Publishing Ltd.

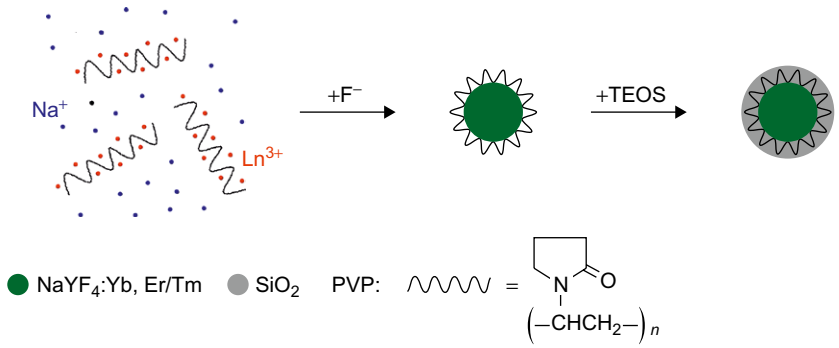

FIGURE 6.3 *Synthesis of silica-coated PVP/$NaYF_4$ nanoparticles doped with lanthanide ions. TEOS = tetraethoxysilane.*

Source: Reproduced with permission from Ref. [49]. Copyright Wiley-VCH Verlag GmbH & Co. KGaA.

for detecting their quantity. Downconverting fluorescence labels suffer from photobleaching, toxicity, low luminescence intensity and decreasing fluorescence intensity in biological fluids[56–58]. The development of biological labels that are resistant to photobleaching, biocompatible, highly luminescent and ultrasensitive in both in vitro and in vivo bioassays remains a

challenging task. Lanthanide doped UCN with NIR excitation can be a good choice[59–61]. These nanoparticles are biocompatible, show high chemical stability and can be used for multiplex imaging. Most importantly, they show very low background signal as the interfering biomolecules in question do not get absorbed in the NIR region. The application of UCN as reporter in homogeneous immunoassays[60–62] and nucleic acid microarrays[63] provides 10–100 folds better detection limits than conventional fluorescence reporters.

Further enhancement in the detection sensitivity can be achieved by introducing UCN coupled with either lateral flow assay or fluorescence resonance energy transfer (FRET). The lateral flow assays are a simple device with a solid substrate, which is pre-treated with antibody or antigen, used for the detection of target analytes in the test sample. UCN based lateral flow assays lead to better detection sensitivity[64, 65]. FRET is one of the most important techniques used to monitor binding interactions based on the detection of proximity between a fluorescent energy donor and an acceptor species. The basic principle of FRET is described as non-radiative energy transfer from a donor to an acceptor species in close proximity with a distance smaller than critical radius known as Forster radius (typically <10 nm)[66]. FRET is a very simple and convenient method. This is used to measure changes in distance rather than the distance itself, thereby making them best suited for measuring protein conformational changes[67], monitoring protein interactions[68] and assaying of enzyme activity[69]. They are based on measurement of either donor quenching or sensitized emission from acceptor. An example for UCN–FRET system for the detection of trace amounts of avidin is shown in Figure 6.4. In this system, biotin conjugated UCN and 7 nm gold nanoparticles were used as energy donor and acceptor, respectively.

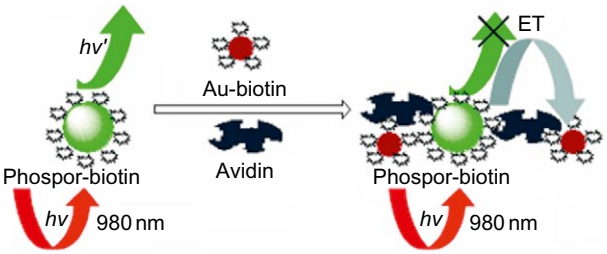

FIGURE 6.4 *Scheme of the FRET system with phosphor-biotin nanoparticles as energy donors and Au-biotin nanoparticles as energy acceptors in the analysis of avidin. ET = energy transfer.*
Source: Reproduced with permission from Ref. [43]. Copyright Wiley-VCH Verlag GmbH & Co. KGaA.

Different concentrations of avidin were added to the mixture of these two nanoparticles and their fluorescent spectra were measured as a function of avidin concentration. It was observed that the luminescence was gradually quenched with increasing amount of avidin[43]. However, UCN–FRET has intrinsic limitations such as large size of UCN and instable conjugation of biomolecules on the surface of UCN. The reduction in size of UCN can increase its signal variation and decrease proximity based energy transfer efficiency. Most efficient energy transfer can be achieved with particles lesser than 40 nm in diameter, in which larger proportion of the emission ions can participate in non-radiative energy transfer due to short distances. The instable conjugation of biomolecules on the surface of UCN is due to the improper coating method that leads to dissociation of bioconjugates from the surface of nanoparticles and decreases their assay sensitivity. Further studies may pave the way to wider applications of these UCN in ultrasensitive multicolour detection of nucleic acids and proteins, and fluorescence immunoassays.

6.5.2 UCN in bioimaging

The morphological and optical properties of nanoparticles are key components for in vitro and in vivo imaging of living cells and animals, respectively. The nanoparticles ought to be compatible in size and chemical composition with the imaging systems. The chemical stability, non-photobleaching and biocompatibility of UCN over conventional labels make them best suitable for bioimaging. UCN of few hundred nanometres were used to image the digestive system of nematode *Caenorhabditis elegans* (*C. elegans*)[70]. Figure 6.5 shows the images of secretion of UCN in digestive system of *C. elegans* under 980 nm excitation. In our lab, PEI stabilized $NaYF_4$ nanoparticles of about 50 nm diameter and with amino functional groups were used for imaging of cells and deep tissues in animals[71]. Folic

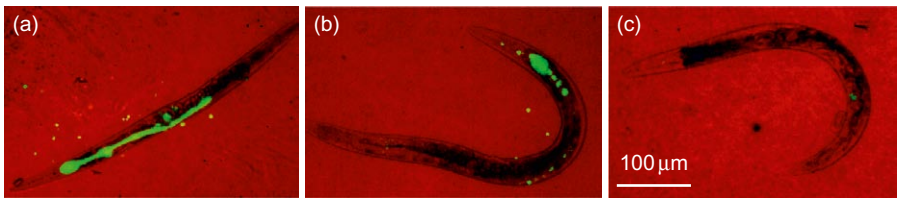

FIGURE 6.5 *False colour two-photon images of C. elegans at 980 nm excitation. The worms were given food immediately after being fed with phosphors, showing decreasing amounts of phosphors at (a) 0 h, (b) 1 h and (c) 2 h.*

Source: Reprinted with permission from Ref. [70]. Copyright 2008, American Chemical Society.

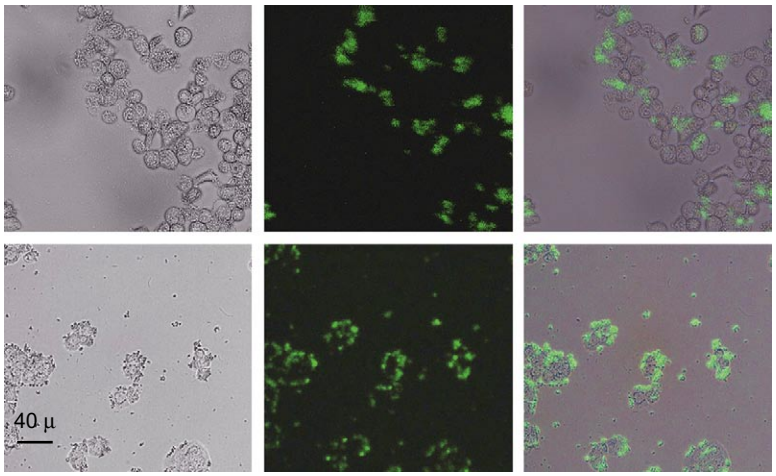

FIGURE 6.6 *Bright field, confocal and superimposed images of live human ovarian carcinoma cells (OVCAR3, top row) and human colonic adenocarcinoma cells (HT29, bottom row), with PEI/$NaYF_4$ nanoparticles attached. The nanoparticles were surface modified with folic acid.*
Source: Reprinted with permission from Ref. [71]. Copyright 2008, Elsevier.

acid coated PEI/$NaYF_4$ nanoparticles were used for imaging human HT29 adenocarcinoma cells and human OVCAR3 ovarian carcinoma cells. The demonstration of its live cellular imaging is shown in Figure 6.6.

The deep tissue imaging of Wistar rats is shown in Figure 6.7. Anaesthetized Wistar rats were injected subcutaneously at groin and upper leg regions with 100 mL of PEI/$NaYF_4$:Yb, Er. The nanoparticles injected show visible fluorescence from a depth of up to 10 mm. The muscles with skin removed show much stronger fluorescence from deep injection than intact skin at similar depths.

In general, the morphological and optical features of UCN make them best suited for continuous live imaging of tissues in small animal models, which can then be utilized in monitoring tumour and exploring pathologies without unnecessary sacrifice of animals. This is particularly important when temporal series of data are required.

6.5.3 UCN for photodynamic therapy

UCN can be administered in therapeutic applications such as photodynamic therapy (PDT). This involves destruction of pathological cells and tissues using toxic oxygen species generated from dynamic interaction of a photosensitizing agent with light and oxygen. This mechanism takes place in three different phases: first, absorption of light by photosensitizing agent

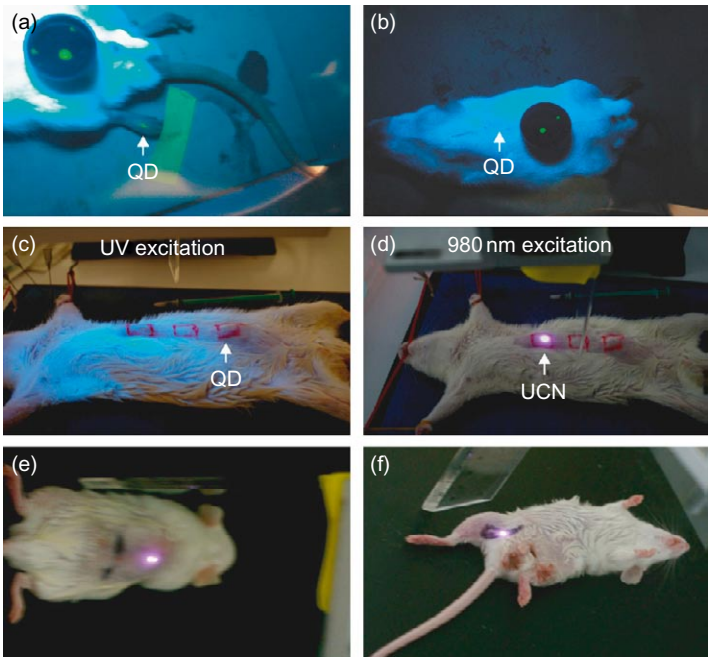

FIGURE 6.7 *In vivo imaging of rat: quantum dots (QDs) injected into translucent skin of foot (a) show fluorescence, but not through thicker skin of back (b) or abdomen (c); PEI/$NaYF_4$:Yb, Er nanoparticles injected below abdominal skin (d), thigh muscles (e) or below skin of back (f) show luminescence. QDs on a black disk in (a) and (b) are used as the control.*
Source: Reprinted with permission from Ref. [71]. Copyright 2008, Elsevier.

to attain an excited state; second, release of energy to surrounding oxygen to convert them to oxygenated products or singlet oxygen and finally, induction of cell death by toxic products. There are some technical difficulties involved in PDT application which decrease their efficiency. They are: (1) most photosensitizers are hydrophobic – they aggregate easily under physical conditions and have low accumulation selectivity towards diseased tissue; (2) photosensitizer absorbs in visible spectral region below 700 nm which cannot penetrate deeply inside tissue. The use of UCN overcomes these drawbacks. UCN by themselves are unable to generate singlet oxygen species from dissolved oxygen and require the attachment of an appropriate photosensitizing agent with excitation band matching the emission of nanoparticles. In principle, incident NIR light is upconverted by UCN to visible light which is used by photosensitizer to produce singlet oxygen species from dissolved molecular oxygen environment. In addition, it helps to solubilize highly non-polar photosensitizer and target them to cancer cells. Accordingly, UCN acts as energy transducer for photosensitizer. UCN,

core-shell silica/$NaYF_4$:Yb, Er with merocyanine-540[72] and PEI/$NaYF_4$:Yb, Er with zinc pthalocyanine [73] are reported for PDT.

6.6 CONCLUSION

Conventional downconverting fluorescent labels suffer from autofluorescence, low light penetration and presence of severe photodamage to living organisms. UCN with NIR laser excitation is a good alternative. Advantages of UCN are strong anti-Stokes emission of discrete wavelengths, unmatched contrast in biological specimens due to the absence of autofluorescence upon excitation with NIR light and simultaneous detection of multiple target analytes. With these advantages, UCN find potential applications in immunoassay, bioimaging[22] and PDT[72, 74]. There is still room for improvement in characteristics of UCN which include its larger size, absence of functional groups for bioconjugations and its instability when dispersed in solutions. In addition, synthesis of bifunctional UCN with both fluorescence and paramagnetic properties has raised a significant interest in the field of biolabelling[75, 76]. These bifunctional nanoparticles have potential application in fluorescence imaging[77], targeting[78], bioseparation, cancer diagnosis and treatment, DNA separation and magnetic resonance imaging (MRI)[79].

ACKNOWLEDGMENTS

The authors acknowledge financial support from A*STAR BMRC (R-397-000-062-305) and the National University of Singapore.

REFERENCES

[1] E. Beaurepaire, V. Buissette, M.P. Sauviat, D. Giaume, K. Lahlil, A. Mercuri, D. Casanova, A. Huignard, J.L. Martin, T. Gacoin, J.P. Boilot, A. Alexandrou, Functionalized fluorescent oxide nanoparticles: Artificial toxins for sodium channel targeting and imaging at the single-molecule level, Nano Lett. 4 (11) (2004) 2079.

[2] K. Konig, Multiphoton microscopy in life sciences, J. Microsc.-Oxford 200 (2000) 83.

[3] G.S. Yi, G.M. Chow, Colloidal LaF3:Yb,Er, LaF3:Yb,Ho and LaF3:Yb,Tm nanocrystals with multicolor upconversion fluorescence, J. Mater. Chem. 15 (41) (2005) 4460.

[4] H. Zijlmans, J. Bonnet, J. Burton, K. Kardos, T. Vail, R.S. Niedbala, H.J. Tanke, Detection of cell and tissue surface antigens using up-converting phosphors: A new reporter technology, Anal. Biochem. 267 (1) (1999) 30.

[5] S. Heer, K. Kompe, H.U. Gudel, M. Haase, Highly efficient multicolour upconversion emission in transparent colloids of lanthanide-doped $NaYF_4$ nanocrystals, Adv. Mater. 16 (23–24) (2004) 2102.

[6] T. Tsuboi, H. Murayama, Energy-transfer upconversion of rare earth ions in ionic crystals: Case of Tm^{3+}/Ho^{3+}-codoped $LiYF_4$ crystals, J. Alloys Compd. 408–412 (2006) 680.

[7] H.W. Song, B.J. Sun, T. Wang, S.Z. Lu, L.M. Yang, B.J. Chen, X.J. Wang, X.G. Kong, Three-photon upconversion luminescence phenomenon for the green levels in Er^{3+}/Yb^{3+} codoped cubic nanocrystalline yttria, Solid State Commun. 132 (6) (2004) 409.

[8] H. Lin, K. Liu, L. Lin, Y. Hou, D. Yang, T. Ma, E.Y.B. Pun, Q. An, J. Yu, S. Tanabe, Optical parameters and upconversion fluorescence in Tm^{3+}/Yb^{3+}-doped alkali–barium–bismuth–tellurite glasses, Spectrochim. Acta A 65 (3–4) (2006) 702.

[9] K. Kadono, H. Higuchi, M. Takahashi, Y. Kawamoto, H. Tanaka, Upconversion luminescence of Ga_2S_3-based sulfide glasses containing Er^{3+} ions, J. Non-Cryst. Solids 184 (1995) 309.

[10] K. Kumar, S.B. Rai, UV/visible upconversion and energy transfer between Nd^{3+} and Pr^{3+} ions in co-doped tellurite glass, Solid State Commun. 142 (1–2) (2007) 58.

[11] M.A. Chamarro, R. Cases, Infrared to visible upconversion of Er^{3+} ions in Yb^{3+} doped fluorohafnate glasses, J. Lumin. 46 (1) (1990) 59.

[12] M. Liao, L. Wen, H. Zhao, Y. Fang, H. Sun, L. Hu, Mechanisms of Yb^{3+} sensitization to Tm^{3+} for blue upconversion luminescence in fluorophosphate glass, Mater. Lett. 61 (2) (2007) 470.

[13] P.V. dos Santos, M.V.D. Vermelho, E.A. Gouveia, M.T. de Araujo, A.S. Gouveia-Neto, F.C. Cassanjes, S.J.L. Ribeiro, Y. Messaddeq, Infrared-to-visible frequency upconversion in Pr^{3+}/Yb^{3+}- and Er^{3+}/Yb^{3+}-codoped tellurite glasses, J. Alloys Compd. 344 (1–2) (2002) 304.

[14] G. Hai, Y. Min, Z. Weiping, Upconversion of Er^{3+} ions in LiKGdF5: Er^{3+}, Dy^{3+} single crystal produced by infrared and green laser, J. Rare Earths 24 (6) (2006) 740.

[15] O.S. Wenger, M. Wermuth, H.U. Gudel, Chemical tuning of transition metal upconversion properties, J. Alloys Compd. 341 (1–2) (2002) 342.

[16] M. Wermuth, H.U. Gudel, Upconversion luminescence in a 5d transition-metal ion system: CsZrCl: Os, Chem. Phys. Lett. 281 (1–3) (1997) 81.

[17] S. Heer, M. Wermuth, K. Kramer, H.U. Gudel, Upconversion excitation of Cr^{3+} 2E emission in $Y_3Ga_5O_{12}$ codoped with Cr^{3+} and Yb^{3+}, Chem. Phys. Lett. 334 (4–6) (2001) 293.

[18] C. Reinhard, K. Kramer, D.A. Biner, H.U. Gudel, V^{3+} sensitized upconversion in $Cs_2NaScC_{l6}:Pr^{3+};V^{3+}$ and $K_2NaScF_6:Er^{3+};V^{3+}$, J. Alloys Compd. 374 (1–2) (2004) 133.

[19] J. Grimm, O.S. Wenger, H.U. Gudel, Broadband green upconversion luminescence of Ni^{2+} in $KZnF_3$, J. Lumin. 102–103 (2003) 380.

[20] S. Heer, K. Petermann, H.U. Gudel, Upconversion excitation of Cr^{3+} emission in $YAlO_3$ codoped with Cr^{3+} and Yb^{3+}, J. Lumin. 102–103 (2003) 144.

[21] T. Hirai, T. Orikoshi, I. Komasawa, Preparation of Y_2O_3 : Yb, Er infrared-to-visible conversion phosphor fine particles using an emulsion liquid membrane system, Chem. Mater. 14 (8) (2002) 3576.

[22] Y. Wei, F.Q. Lu, X.R. Zhang, D.P. Chen, Synthesis and characterization of efficient near-infrared upconversion Yb and Tm codoped $NaYF_4$ nanocrystal reporter, J. Alloys Compd. 427 (1–2) (2007) 333.

[23] H. Guo, N. Dong, M. Yin, W. Zhang, L. Lou, S. Xia, Green and red upconversion luminescence in Er^{3+}-doped and Er^{3+}/Yb^{3+}-codoped $SrTiO_3$ ultrafine powders, J. Alloys Compd. 415 (1–2) (2006) 280.

[24] Y. Wei, F. Lu, X. Zhang, D. Chen, Synthesis and characterization of efficient near-infrared upconversion Yb and Tm codoped $NaYF_4$ nanocrystal reporter, J. Alloys Compd. 427 (1–2) (2007) 333.

[25] Y. Kuisheng, L. Yan, Y. Chaoyi, L. Liping, Y. Chanhua, Z. Xiyan, Upconversion luminescence properties of Ho^{3+}, Tm^{3+}, Yb^{3+} co-doped nanocrystal $NaYF_4$ synthesized by hydrothermal method, J. Rare Earths 24 (6) (2006) 757.

[26] T. Hirai, T. Orikoshi, Preparation of yttrium oxysulfide phosphor nanoparticles with infrared-to-green and -blue upconversion emission using an emulsion liquid membrane system, J. Colloid Interface Sci. 273 (2) (2004) 470.

[27] H.U. Gudel, M. Pollnau, Near-infrared to visible photon upconversion processes in lanthanide doped chloride, bromide and iodide lattices, J. Alloys Compd. 303–304 (2000) 307.

[28] R.X. Yan, Y.D. Li, Down/up conversion in $Ln^{(3+)}$-doped YF_3 nanocrystals, Adv. Funct. Mater. 15 (5) (2005) 763.

[29] X.P. Fan, D.B. Pi, F. Wang, J.R. Qiu, M.Q. Wang, Hydrothermal synthesis and luminescence behavior of lanthanide-doped GdF_3 nanoparticles, IEEE Trans. Nanotechnol. 5 (2) (2006) 123.

[30] G.S. Yi, H.C. Lu, S.Y. Zhao, G. Yue, W.J. Yang, D.P. Chen, L.H. Guo, Synthesis, characterization, and biological application of size-controlled nanocrystalline $NaYF_4$: Yb,Er infrared-to-visible up-conversion phosphors, Nano Lett. 4 (11) (2004) 2191.

[31] G.S. Yi, G.M. Chow, Colloidal LaF_3 : Yb,Er, LaF_3 : Yb,Ho and LaF_3 : Yb,Tm nanocrystals with multicolor upconversion fluorescence, J. Mater. Chem. 15 (41) (2005) 4460.

[32] T. Hirai, T. Orikoshi, Preparation of Gd_2O_3 : Yb,Er and Gd2O2S : Yb,Er infrared-to-visible conversion phosphor ultrafine particles using an emulsion liquid membrane system, J. Colloid Interface Sci. 269 (1) (2004) 103.

[33] G.S. Yi, B.Q. Sun, F.Z. Yang, D.P. Chen, Y.X. Zhou, J. Cheng, Synthesis and characterization of high-efficiency nanocrystal up-conversion phosphors: ytterbium and erbium codoped lanthanum molybdate, Chem. Mater. 14 (7) (2002) 2910.

[34] X. Wang, X.G. Kong, G.Y. Shan, Y. Yu, Y.J. Sun, L.Y. Feng, K.F. Chao, S.Z. Lu, Y.J. Li, Luminescence spectroscopy and visible upconversion properties of Er^{3+} in ZnO nanocrystals, J. Phys. Chem. B 108 (48) (2004) 18408.

[35] A. Walasek, Z. Eugeniusz, J. Zhang, S.W. Wang, Synthesis, morphology and spectroscopy of cubicY(3)NbO(7): Er, J. Lumin. 127 (2) (2007) 523.

[36] L. An., J. Zhang, M. Lui, S. Wang, Preparation and upconversion properties of Yb^{3+},Ho^{3+}:Lu_2O_3 nanocrystalline powders, J. Am. Ceram. Soc. 88 (4) (2005) 1010.

[37] D. Wang, Y. Guo, G. Sun, J. Li, L. Zhao, G. Xu, Blue, green, yellow and red upconversion fluorescence in Tm^{3+}/Ho^{3+}:$Cs_2NaGdCl_6$ crystals under 785 nm laser excitation, J. Alloys Compd. 451 (1–2) (2008) 122.

[38] D.S. Jacob, L. Bitton, J. Grinblat, I. Felner, Y. Koltypin, A. Gedanken, Are ionic liquids really a boon for the synthesis of inorganic materials? A general method for the fabrication of nanosized metal fluorides, Chem. Mater. 18 (13) (2006) 3162.

[39] K.L. Wong, G.L. Law, W.M. Kwok, W.T. Wong, and D.L. Phillips, Simultaneous observation of green multiphoton upconversion and red and blue NLO process from polymeric terbium(III)complexes, Angew. Chem. Int. Ed. 44 (2005) 3436.

[40] K.L. Wong, W.M. Kwok, W.T. Wong, D.L. Phillips, K.W. Cheah, Green and red three-photon upconversion from polymeric lanthanide complexes, Angew. Chem. Int. Ed. 43 (2004) 4659.

[41] J.H. Zeng, J. Su, Z.H. Li, R.X. Yan, Y.D. Li, Synthesis and upconversion luminescence of hexagonal-phase $NaYF_4$: Yb, Er^{3+}, phosphors of controlled size and morphology, Adv. Mater. 17 (17) (2005) 2119.

[42] S. Heer, O. Lehmann, M. Haase, H.U. Gudel, Blue, green, and red upconversion emission from lanthanide-doped $LuPO_4$ and $YbPO_4$ nanocrystals in a transparent colloidal solution, Angew. Chem. Int. Ed. 42 (27) (2003) 3179.

[43] L.Y. Wang, R.X. Yan, Z.Y. Hao, L. Wang, J.H. Zeng, H. Bao, X. Wang, Q. Peng, Y.D. Li, Fluorescence resonant energy transfer biosensor based on upconversion-luminescent nanoparticles, Angew. Chem. Int. Ed. 44 (37) (2005) 6054.

[44] V. Sudarsan, S. Sivakumar, F. van Veggel, M. Raudsepp, General and convenient method for making highly luminescent sol–gel derived silica and alumina films by using LaF_3 nanoparticles doped with lanthanide ions (Er^{3+}, Nd^{3+}, and Ho^{3+}), Chem. Mater. 17 (18) (2005) 4736.

[45] J. Xue, C. Wang, Z. Ma, A facile method to prepare a series of SiO_2@Au core/shell structured nanoparticles, Mater. Chem. Phys. 105 (2–3) (2007) 419.

[46] G.Z.Y.M. Li, Z.L. Wang, J. Lin, R.S. Wang, J. Fang, Sol–gel fabrication and photoluminescence properties of SiO_2 @ Gd_2O_3:Eu^{3+} core-shell particles, J. Nanosci. Nanotechnol. 6 (5) (2006) 1416.

[47] H.Y.M. Wang, C.K. Lin, J. Lin, Core-shell structured SiO_2@YVO_4:Dy^{3+}/Sm^{3+} phosphor particles: Sol–gel preparation and characterization, J. Colloid. Interface Sci. 300 (1) (2006) 176.

[48] A. Wolcott, D. Gerion, M. Visconte, J. Sun, A. Schwartzberg, S.W. Chen, J.Z. Zhang, Silica-coated CdTe quantum dots functionalized with thiols for bioconjugation to IgG proteins, J. Phys. Chem. B 110 (11) (2006) 5779.

[49] Z.Q. Li, Y. Zhang, Monodisperse silica-coated polyvinylpyrrolidone/$NaYF_4$ nanocrystals with multicolor upconversion fluorescence emission, Angew. Chem. Int. Ed. 45 (46) (2006) 7732.

[50] M. Kumar, A review of chitin and chitosan applications, React. Funct. Polym. 46 (1) (2000) 1.

[51] S. Miyazaki, K. Ishii, T. Nadai, The use of chitin and chitosan as drug carriers, Chem. Pharm. Bull. 29 (10) (1981) 3067.

[52] W.B. Tan, Y. Zhang, Surface modification of gold and quantum dot nanoparticles with chitosan for bioapplications, J. Biomed. Mater. Res. A 75A (1) (2005) 56.

[53] F. Wang, D.K. Chatterjee, Z.Q. Li, Y. Zhang, X.P. Fan, M.Q. Wang, Synthesis of polyethylenimine/$NaYF_4$ nanoparticles with upconversion fluorescence, Nanotechnology 17 (23) (2006) 5786.

[54] T. Konishi, K. Shimizu, Y. Saito, K. Saga, Surface modification of upconversion nanophosphors with poly(acrylic acid), J. Photopolym. Sci. Technol. 20 (1) (2007) 11.

[55] T. Konishi, M. Yamada, K. Soga, D. Matsuura, Y. Nagasaki, PEG-based surface modification on upconversion nanophosphors for bio-imaging under IR excitation, J. Photopolym. Sci. Technol. 19 (2) (2006) 145.

[56] W.C.Y. Pham, R. Weissleder, C.H. Tung, Developing a peptide based near-infrared molecular probe for protease sensing, Bioconjugate Chem. 15 (2004) 1403.

[57] S.M.P.S. Messerli, Y. Tang, K. Shah, M.L. Cortes, V. Murthy, et al., A novel method for imaging apoptosis using a caspase-1 near-infrared fluorescent probe, Neoplasia 6 (2004) 95.

[58] C.R.M.C. Kagan, M. Nirmal, M.G. Bawendi, Electronic energy transfer in CdSe quantum dot solids, Phys. Rev. Lett. 76 (1996) 1517.

[59] C.G. Morgan, A.C. Mitchell, Prospects for applications of lanthanide-based upconverting surfaces to bioassay and detection, Biosens. Bioelectron. 22 (8) (2007) 1769.

[60] K. Kuningas, T. Rantanen, T. Ukonaho, T. Lovgren, T. Soukka, Homogeneous assay technology based on upconverting phosphors, Anal. Chem. 77 (22) (2005) 7348.

[61] K. Kuningas, T. Ukonaho, H. Pakkila, T. Rantanen, J. Rosenberg, T. Lovgren, T. Soukka, Upconversion fluorescence resonance energy transfer in a homogeneous immunoassay for estradiol, Anal. Chem. 78 (13) (2006) 4690.

[62] K. Kuningas, H. Pakkila, T. Ukonaho, T. Rantanen, T. Lovgren, T. Soukka, Upconversion fluorescence enables homogeneous immunoassay in whole blood, Clin. Chem. 53 (1) (2007) 145.

[63] F. van de Rijke, H. Zijlmans, S. Li, T. Vail, A.K. Raap, R.S. Niedbala, H.J. Tanke, Up-converting phosphor reporters for nucleic acid microarrays, Nat. Biotechnol. 19 (3) (2001) 273.

[64] P. Corstjens, M. Zuiderwijk, A. Brink, S. Li, H. Feindt, R.S. Neidbala, H. Tanke, Use of up-converting phosphor reporters in lateral-flow assays to detect specific nucleic acid sequences: A rapid, sensitive DNA test to identify human papillomavirus type 16 infection, Clin. Chem. 47 (10) (2001) 1885.

[65] P. Corstjens, M. Zuiderwijk, M. Nilsson, H. Feindt, R.S. Niedbala, H.J. Tanke, Lateral-flow and up-converting phosphor reporters to detect single-stranded nucleic acids in a sandwich-hybridization assay, Anal. Biochem. 312 (2) (2003) 191.

[66] J.N.T. Riegler, Application of luminescent nanocrystals as labels for biological molecules, Anal. Bioanal. Chem. 379 (2004) 913.

[67] T. Heyduk, Measuring protein conformational changes by FRET/LRET, Curr. Opin. Biotechnol. 13 (2002) 292.

[68] R.N.P.A. Day, F. Schaufele, Fluorescence resonance energy transfer microscopy of localized protein interactions in the living cell nucleus, Methods 25 (2001) 4.

[69] J.J.B.T. Li, A fluorescent analogue of UDP-N-acetylglucosamine:application for FRET assay of peptidoglycan translocase (MurG), Chem. Commun. 182 (2004).

[70] S.F. Lim, R. Riehn, W.S. Ryu, N. Khanarian, C.K. Tung, D. Tank, R.H. Austin, In vivo and scanning electron microscopy imaging of upconverting nanophosphors in *Caenorhabditis elegans*, Nano Lett. 6 (2) (2006) 169.

[71] D.K. Chatteriee, A.J. Rufalhah, Y. Zhang, Upconversion fluorescence imaging of cells and small animals using lanthanide doped nanocrystals, Biomaterials 29 (7) (2008) 937.

[72] P. Zhang, W. Steelant, M. Kumar, M. Scholfield, Versatile photosensitizers for photodynamic therapy at infrared excitation, J. Am. Chem. Soc. 129 (15) (2007) 4526.

[73] D.K. Chatterjee, Y. Zhang, Upconverting nanoparticles as nanotransducers for photodynamic therapy in cancer cells, Nanomedicine 3 (1) (2008) 73.

[74] X. Qin, T. Yokomori, Y.G. Ju, Flame synthesis and characterization of rare-earth (Er^{3+}, Ho^{3+}, and Tm^{3+}) doped upconversion nanophosphors, Appl. Phys. Lett. 90 (7) (2007).

[75] S.Y.Z.H. Yu, J.B. Yu, C. Wang, L.N. Sun, W.D. Shi, Bifunctional magnetic–optical nanocomposites: grafting lanthanide complex onto core-shell magnetic silica nanoarchitecture, Langmuir 23 (14) (2007) 7836.

[76] Z.Y. Liu, G.S. Yi, H.T. Zhang, J. Ding, Y.W. Zhang, J.M. Xue, Monodisperse silica nanoparticles encapsulating upconversion fluorescent and superparamagnetic nanocrystals, Chem. Commun. (6) (2008) 694.

[77] J. Wu, Z.Q. Ye, G.L. Wang, J.L. Yuan, Multifunctional nanoparticles possessing magnetic, long-lived fluorescence and bio-affinity properties for time-resolved fluorescence cell imaging, Talanta 72 (5) (2007) 1693.

[78] O. Veiseh, C. Sun, J. Gunn, N. Kohler, P. Gabikian, D. Lee, N. Bhattarai, R. Ellenbogen, R. Sze, A. Hallahan, J. Olson, M.Q. Zhang, Optical and MRI multifunctional nanoprobe for targeting gliomas, Nano Lett. 5 (6) (2005) 1003.

[79] W.B. Tan, Y. Zhang, Multi-functional chitosan nanoparticles encapsulating quantum dots and Gd-DTPA as imaging probes for bio-applications, J. Nanosci. Nanotechnol. 7 (7) (2007) 2389.